HHS Public Access

Author manuscript

Sci Immunol. Author manuscript; available in PMC 2019 September 30.

Published in final edited form as:

Sci Immunol. 2019 May 03; 4(35): . doi:10.1126/sciimmunol.aax0416.

Stromal Cells Maintain Immune Cell Homeostasis in Adipose Tissue via Production of Interleukin-33

T. Mahlakõiv[1], **A.-L. Flamar**[1], **L. K. Johnston**[2,4], **S. Moriyama**[1,5], **G. G. Putzel**[1], **P. J. Bryce**[2,3], **D. Artis**[1,*]

[1]Jill Roberts Institute for Research in Inflammatory Bowel Disease, Joan and Sanford I. Weill Department of Medicine, Department of Microbiology and Immunology, Weill Cornell Medicine, Cornell University, New York, NY 10021, USA.

[2]Division of Allergy-Immunology, Department of Medicine, Feinberg School of Medicine, Northwestern University, Chicago, IL 60610, USA.

[3]Current address: Immunology & Inflammation Therapeutic Area, Sanofi US, Cambridge, MA 02139, USA.

[4]Current address: Cytometry and Antibody Technology Facility, University of Chicago, Chicago, IL 60637, USA.

[5]Current address: Department of Immunology, National Institute of Infectious Diseases, Shinjuku, Tokyo, 162-8640, Japan.

Abstract

Obesity is driven by chronic low-grade inflammation resulting from dysregulated immune cell accumulation and function in white adipose tissue (WAT). Interleukin-33 (IL-33) is a key cytokine that controls innate and adaptive immune cell activity and immune homeostasis in WAT, although the sources of IL-33 have remained controversial. Here, we show that WAT-resident mesenchyme-derived stromal cells are the dominant producers of IL-33. Adipose stem and progenitor cells (ASPCs) produced IL-33 in all WAT depots, whereas mesothelial cells served as an additional source of IL-33 in visceral WAT. ASPC-derived IL-33 promoted a regulatory circuit that maintained immune tone in WAT via the induction of group 2 innate lymphoid cell-derived type 2 cytokines and maintenance of eosinophils, while mesothelial IL-33 also acted as an alarmin by inducing peritoneal immune response upon infection. Together, these data reveal a previously unrecognized regulatory network between tissue-resident progenitor cells and innate lymphoid cells that maintains immune homeostasis in adipose tissue.

*Corresponding author: dartis@med.cornell.edu.

Author contributions: D.A. and T.M. conceived the project and wrote the manuscript with input from all co-authors. T.M. performed the experiments and analyzed the data with help from A-L.F. and S.M. P.B. and L.J. generated the IL-33-eGFP mouse. G.G.P. analyzed the RNAseq data. T.M. compiled the data and performed statistical analysis.

Competing Interests: D.A. has contributed to scientific advisory boards at FARE, KRF, MedImmune and Pfizer. P. B. generated the IL-33-eGFP mouse while an employee at Northwestern University but is currently an employee of Sanofi US, who was not involved in this study. All other authors declare that they have no competing interests.

Data and Materials Availability: The RNAseq data was deposited in the GEO database under accession number GSE129065. All other data needed to evaluate the conclusions in the paper are present in the paper or the Supplementary Materials.

One Sentence Summary:

Tissue-resident stromal cells control innate lymphoid cell-dependent immune homeostasis in adipose tissue.

Introduction

The global pandemic of obesity and obesity-related co-morbidities continues to escalate at an alarming rate. Currently, more than 2 billion people worldwide are overweight or obese (1). Increased white adipose tissue (WAT) mass, accompanied by chronic low-grade inflammation, is a major risk factor of cardiovascular diseases and predisposes to the development of type 2 diabetes, hypertension, hyperlipidemia and certain cancers, which altogether impose an enormous burden on the public health care system and the economy (2). WAT is densely populated by various immune cells that maintain metabolic homeostasis and become dysregulated in obesity (3). Genetic variations in interleukin-33 (IL-33), a critical immunomodulatory alarmin, have previously been linked to the development of obesity in humans, suggesting a regulatory role for IL-33 in the control of adipose tissue immune responses and subsequent metabolic health (4, 5). Accordingly, in humans, circulating IL-33 levels are negatively correlated with body mass index and adiposity (6).

The receptor for IL-33, termed ST2, is highly expressed on the anti-inflammatory cells in lean WAT, including group 2 innate lymphoid cells (ILC2s) and regulatory T cells (Tregs), which maintain eosinophil numbers and promote an anti-inflammatory phenotype in macrophages (7–12). The metabolically beneficial effect of IL-33 has been linked to increased type 2 cytokine production by WAT ILC2s (12–14). Accordingly, IL-33 signaling deficiency in mice results in increased adipose tissue, body mass, and WAT inflammation, whereas IL-33 treatment boosts the numbers and activity of WAT ILC2s, Tregs and eosinophils (7, 12, 13, 15).

Despite our growing understanding of the role of IL-33 in regulating WAT immune balance and homeostasis, the cellular sources and molecular mechanisms controlling these processes in WAT remain incompletely understood. In the intestine and the lung, where IL-33 serves as an alarmin by inducing type 2 inflammation upon tissue damage, IL-33 is known to be constitutively expressed in the nucleus of epithelial cells, endothelial cells and fibroblasts (16–21). Additionally, under certain inflammatory conditions, IL-33 has also been reported to be expressed by several hematopoietic cell lineages, including mast cells, macrophages and dendritic cells (22, 23).

Results

IL-33 regulates ILC2 activity and eosinophil numbers

We sought to identify the cell types that produce IL-33 and control immunological homeostasis in WAT. We first characterized the immunological consequences of IL-33 deficiency in mice. As reported, IL-33 deficiency in mice resulted in spontaneous weight gain and increased adiposity (Fig. 1A–C) (7). We next analyzed the immune cell phenotype in IL-33-deficient animals (*Il33*$^{-/-}$) in visceral WAT depots (epididymal, ewat and the

mesenteric, mwat) that drive the inflammatory process in human obesity. Notably, we found that ILC2s accumulate more in visceral WAT, specifically in mwat, compared to subcutaneous WAT (inguinal, iwat) (fig. S1A; ILC2 gating demonstrated in fig. S9A). ILC2 numbers in visceral WAT were not affected in IL-33-deficient animals at steady state (Fig. 1D), although they exhibited reduced capacity to produce type 2 cytokines, including IL-5, which is known to sustain WAT eosinophils (Fig. 1E and 1F) (13). Additionally, IL-33 deficiency in mice resulted in severely decreased eosinophil but not macrophage numbers in visceral WAT (Fig. 1G and 1H; gating demonstrated in fig. S9B) (13). A similar dysregulated immune cell phenotype was also observed in animals lacking a functional IL-33 receptor (*Il1rl1*$^{-/-}$) (Fig. S1B–E). In agreement with these findings, administration of recombinant IL-33 to IL-33-deficient animals boosted type 2 cytokine production by ILC2s and restored WAT eosinophil numbers (Fig. S2A–2D).

Visceral WAT adipose stem and progenitor cells produce IL-33

Our finding that IL-33 regulates weight gain, adiposity, and WAT immune cell infiltrates supports an established role for IL-33 in WAT homeostasis. Yet, whereas IL-33 has been reported to regulate WAT composition and inflammation, the identity of IL-33-producing cells in WAT has remained elusive. To this end, we undertook a comprehensive and unbiased analysis of WAT-resident IL-33-producing cells. First, whole eWAT was enzymatically digested and separated into adipocytes and the stromal vascular fraction (SVF), and the latter further separated by cell sorting into hematopoietic (CD45^{+}) or non-hematopoietic cell (CD45^{-}) fractions. Relative expression analysis of adipocyte and SVF fractions by quantitative real-time reverse transcription PCR (qRT-PCR) revealed high *Il33* transcript expression in SVF, particularly in non-hematopoietic cells (CD45^{-}), but undetectable levels in adipocytes (Fig. 2A and 2B and fig. S3A).

Further analysis of IL-33 expression by flow cytometry demonstrated that IL-33 protein was predominantly expressed in SVF cells lacking the hematopoietic, endothelial, and erythroid cell markers CD45, CD31, and Ter119, respectively (termed lineage negative; lin^{-}), but expressing stromal cell markers Sca-1 and platelet-derived growth factor receptor α (PDGFRα) (Fig. 2C). To further characterize the stromal cell population expressing IL-33, we performed RNA sequencing (RNAseq) on sorted lin^{-} Sca-1^{+} PDGFRα^{+} WAT cells. RNAseq demonstrated relatively high expression of genes associated with adipose stem and progenitor cells (ASPCs), including *Pdgfra, Ly6a* (Sca-1), *Itgb1* (CD29), *Pdpn* and *Cd34*, and an array of immune-related genes (Fig. 1D, fig. S4A and S4B). *Il33* was among the highest expressed immune-related genes in ASPCs (Fig S4A and S4B). qRT-PCR analysis confirmed high *Il33* transcript expression in sort-purified ASPCs compared to adipocytes, hematopoietic or endothelial cells (Fig. 2E), and nuclear IL-33 protein expression was observed in sort-purified cultured ASPCs (fig. S3B). Whereas the majority of IL-33^{+} cells were ASPCs (approximately 90% of the lin^{-} population), IL-33 was expressed in 43% of total ASPCs (fig. S3C, right panel). ASPCs formed a large population of total live WAT SVF cells (fig. S3C), suggesting their prominent role in shaping the immunomodulatory environment in WAT via IL-33.

To characterize the IL-33-producing cells in more detail, we generated an IL-33-eGFP reporter mouse expressing enhanced green fluorescent protein (eGFP) under the control of the *Il33* gene promoter. A majority (75%) of the eGFP$^+$ cells in the SVF expressed the ASPC markers Sca-1 and PDGFRα (Fig. 2F), validating the IL-33 antibody staining (Fig. 2C and S3C). Furthermore, qRT-PCR analysis confirmed high *Il33* transcript expression in sort-purified eGFP$^+$ ASPCs, whereas *Pdgfra* was expressed on both eGFP$^+$ and eGFP$^-$ ASPCs (fig. S3D). Using single-cell RNAseq, it was recently demonstrated that ASPCs comprise several subsets characterized as Ly6C$^+$ fibro-inflammatory progenitors and Ly6C$^-$ CD9$^-$ adipocyte precursor cells (24). *Il33* transcript and eGFP$^+$ were detectable in the three dominant ASPC subsets, as identified by CD9 and Ly6C expression (Fig. 2F and fig. S3E, S3F, S3J).

Whereas ASPCs formed a dominant cell population expressing IL-33 in visceral WAT, eGFP was also expressed in a smaller (approximately 15% of eGFP$^+$) lin$^-$ population lacking PDGFRα (Fig. 2F). Flow cytometry characterization of the eGFP$^+$ cells using an array of stromal cell markers allowed the discrimination of an eGFP$^+$ lin$^-$ podoplanin (PDPN)^{hi} CD9$^+$ PDGFRα$^-$ cell population reminiscent of mesothelial cells (Fig. 2G, fig. S3G and S3H) (24). In contrast to ASPCs, these cells demonstrated a strong eGFP signal in the majority of the population (Fig. 2G and fig S3J). Furthermore, we observed high expression of the mesothelium-specific genes *Msln*, *Lrrn4* and *Upk3b* in sort-purified PDGFRα$^-$ PDPN$^+$ cells, but not in ASPCs, which highly expressed *Pdgfra* and *Ccl11*, confirming that mesothelial cells represent a distinct IL-33-expressing cell population in visceral WAT (Fig. 2H, fig S3H and S3I).

Mesothelial cells line the pericardial, pleural, and peritoneal body cavities and surround the organs within, including the visceral adipose compartments (25). Accordingly, mesothelin (MSLN)-stained mesothelial cells were present only in visceral WAT depots (eWAT and mwat), but not in the subcutaneous WAT (iwat) compartment, which has a distinct developmental origin from visceral WAT depots (Fig. 2I) (26). The iwat compartment, however, included a large population of ASPCs of which a high proportion was eGFP$^+$ (Fig 2I, 2J, fig. S5A and S5B). Analysis of additional WAT depots revealed that ASPCs populated all WAT depots in the body and approximately 40–70% were eGFP$^+$, indicating that ASPCs are the dominant IL-33-producing cell type in body WAT (Fig 2J, fig. S5A and S5B).

ASPCs are scattered between adipocytes and the mesothelium envelops the visceral WAT depot

We next sought to visualize the localization of IL-33-producing cells in WAT utilizing the IL-33-eGFP reporter mouse. eGFP$^+$ cells were readily detectable by fluorescence microscopy throughout all WAT compartments (Fig. 3A and fig. S6A). To visualize IL-33-producing cells in more detail, we performed antibody staining of paraffin-embedded tissue sections. Nuclear IL-33 staining was intermittently detectable among adipocytes and in a thin layer of PDPN$^+$ cells lining the perilipin-marked adipocyte mass (Fig. 3B). Because adipocytes did not express meaningful levels of *Il33* (Fig. 2A and 2E), these IL-33$^+$ cells likely represented ASPCs. In support of this, PDGFRα-stained cells were found embedded

between adipocytes (Fig. 3C). To better visualize the three-dimensional tissue morphology and preserve optimal antigen integrity, we performed whole mount tissue staining on WAT. IL-33-expressing PDPN$^+$ PDGFRα$^+$ were interspersed between adipocytes throughout the adipose compartment, consistent with ASPC identity (Fig. 3D). IL-33 staining was also evident in the nuclei of PDPN$^+$ cobblestone-shaped cells, which form the simple squamous epithelium-like layer around the visceral WAT compartment (Fig. 3D and 3E). The location and morphology of these cells suggested mesothelial cells that arise from the mesoderm and express both epithelial and mesenchymal markers (25). Immunostaining for the epithelial tight junction protein ZO-1 and Wilms tumor factor-1 (WT1), a transcription factor expressed in mesoderm-derived tissues, supported the mesothelial nature of the IL-33$^+$ cells (Fig. 3F and 3G). Collectively, these data demonstrate the existence of two mesoderm-derived cell types in visceral WAT expressing IL-33, including an ASPC population scattered between adipocytes and the mesothelium that envelops the visceral WAT depot.

Due to distinct morphology, location, evolutionary origin and function of the visceral and subcutaneous WAT compartments, we also visualized IL-33-producing cells in mwat, a major visceral WAT compartment, and the subcutaneous iwat. Antibody staining of paraffin-embedded tissue sections and whole mount tissues both demonstrated large IL-33-expressing membrane-like structures in the mesentery composed of a double-layer of mesothelial cells (PDPN$^+$) enveloping PDGFRα$^+$ ASPCs (fig. S6B, S6C and S6E). In iwat, large areas of PDPN$^+$ PDGFRα$^+$ ASPCs localized to the periphery of the depot, demonstrating that the majority of ASPCs are not embedded between adipocytes but reside in the fascia, the connective tissue under the skin that extends throughout the body (fig. S6B, S6C, S6D and S6F). A large proportion of these spindle-shaped ASPCs surrounding iwat expressed nuclear IL-33 (fig. S6C and S6D). Together, these data demonstrate that IL-33-expressing ASPCs populate all WAT compartments in the body, including the connective tissue under the skin, suggesting that ASPCs play an important role in IL-33-dependent immune homeostasis in body WAT.

Flow cytometric analysis of visceral WAT from a healthy human donor demonstrated IL-33 protein expression predominantly in lin$^-$ cells expressing Sca-1 and PDGFRα as seen in mice (fig. S7A). Furthermore, IL-33 staining of paraffin-embedded human visceral WAT sections revealed IL-33 positive nuclei interspersed between perilipin$^+$ adipocytes (fig. S7B). These data suggest that the capacity of ASPCs to produce IL-33 is conserved in mice and humans.

Adipose stem and progenitor cell-derived IL-33 controls ILC2 activity

IL-33 is known to control the function of both ILC2s and Tregs (the latter the focus of an accompanying manuscript from Mathis and colleagues) in multiple tissues (27, 46). Suggestive of an ILC2-dependent role for ASPC-derived IL-33, we observed that the majority of lymphocytes expressing the IL-33 receptor component ST2 in WAT were ILC2s (Fig. 4A). Furthermore, compared to small intestinal lamina propria (SI LP) ILC2s, ewat ILC2s expressed ST2 at a much higher level (Fig. 4B and 4C). To study the potential interaction of WAT ILC2s and ASPCs, we stimulated ILC2s *in vitro* with ASPC-conditioned medium (Fig. 4D). Remarkably, upon WAT ILC2 stimulation with ASPC-conditioned

medium, only wild type (WT) ILC2s, but not ST2-deficient (*Il1rl1*$^{-/-}$) ILC2s, secreted IL-5, indicating that ASPCs stimulated ILC2s in an ST2-dependent manner (Fig. 4E). Furthermore, ILC2s from SI LP, which express lower levels of ST2 (Fig. 4B and 4C), secreted less of the type 2 cytokines IL-5 and IL-13 in response to ASPC-conditioned medium (Fig. 4F). Next, we tested whether transfer of wild type ASPCs into IL-33-deficient animals could rescue defective ILC2 and eosinophil responses in WAT (Fig. 1 and Fig. 4G). In agreement with an ASPC- and ILC2-dependent mechanism of action, *Il33*$^{-/-}$ mice receiving adoptively transferred WT ASPCs, but not *Il33*$^{-/-}$ ASPCs, exhibited increased numbers of ILC2s in WAT that produced type 2 cytokines (Fig. 4H and 4I). The transfer of ASPCs also significantly increased eosinophil numbers and proportions in WAT (Fig. 4J). Together, these data demonstrate that ASPCs regulate the cytokine milieu and cellular composition of WAT via IL-33 production.

IL-33 controls adipose tissue expansion and immunological homeostasis in short-term HFD feeding

IL-33 has been implicated in the control of high fat diet (HFD)-induced obesity; however, its role in the acute regulation of WAT inflammation and immune cell homeostasis has not been studied (7, 12, 15). In order to study the cellular composition and immunological changes during acute weight gain, we fed mice with HFD. Rapid body weight gain and accumulation of WAT was seen after only a few days on HFD (fig. S8A and 8B). Moreover, rapid proliferation (Ki67^{+}) of ASPC in visceral but not subcutaneous WAT compartments was observed in HFD versus control diet (CD)-fed mice, that likely contributed to increased lipid storage in HFD-fed mice (Fig. 5A and 5B), as previously reported (28). Notably, when expression of *Il33* was assessed, we found that short-term HFD induced a sharp decrease in *Il33* transcript in ASPCs but not in mesothelial cells (Fig. 5C and fig. S8C). Furthermore, we found that decreased *Il33* expression was accompanied by increased expression of the pro-inflammatory chemokine *Mcp1* (CCL2) in both sort-purified ASPCs and mesothelial cells (Fig. 5C and fig. S8C), indicating rapid immunological changes in the tissue microenvironment.

We next analyzed the effect of loss of IL-33 on short-term HFD feeding-induced immunologic changes in WAT. Strikingly, *Il33*$^{-/-}$ mice displayed elevated weight gain and visceral WAT mass compared to their wild type counterparts after only 3 days of HFD feeding (Fig. 5D and 5E). Increased weight gain was paralleled by a significant increase in Ki67^{+} ASPCs and an increased frequency of CD24^{+} adipose progenitor cells, which promote WAT growth through the generation of new adipocytes (Fig. 5F and fig. S8D) (29, 30). ASPCs in *Il33*$^{-/-}$ mice also exhibited increased size and granularity, further supporting WAT mass accumulation in IL-33-deficient animals compared to WT mice (Fig. 5G).

Accumulation of adipose tissue mass is known to be accompanied by increased levels of baseline inflammation (2). IL-33 has been reported to control inflammatory macrophage homeostasis in WAT by regulating production of type 2 cytokines, including IL-5 and IL-4 secreted by ILC2s and eosinophils, respectively (3). Whereas eosinophil numbers remained constant in mice fed with HFD for 3 days, we observed significantly increased numbers and proportions of macrophages and dendritic cells in *Il33*$^{-/-}$ mice, indicating WAT

inflammation may rapidly develop following HFD feeding in the absence of IL-33 (Fig. 5H, 5I and fig. S8E). These metabolic changes were recapitulated in the ST2-deficient mice (*Il1rl1*$^{-/-}$) (fig. S8F and S8G), further strengthening the importance of the IL-33 pathway in the maintenance of WAT homeostasis. Together, these data support a model in which ASPC-derived IL-33 decreases with the onset of obesity, and subsequently enables a switch towards a pro-inflammatory milieu in WAT.

Mesothelial IL-33 acts as an alarmin to activate the immune system upon peritoneal infection

In addition to ASPCs, we observed that IL-33 was also present in the mesothelial membrane that lines visceral organs and body cavities (Fig. 3) (25). Given the influence of ASPC-derived IL-33 on immune cell homeostasis, we hypothesized that IL-33 in the epithelium-like membrane might serve alarmin functions in response to damage or peritoneal infection, as it is known to operate in other tissues such as the intestine (31). Consistent with this hypothesis, intraperitoneal challenge with an intestinal helminth parasite *Nippostrongylus brasiliensis* (*N.b.*) induced a rapid relocalization of IL-33 from the nucleus of mesothelial cells to the cytoplasm, and IL-33 was also detectable in the peritoneal lavage fluid and serum of *N.b.*-infected mice (Fig. 6A and 6B). Since we also detected rapid secretion of IL-5 in the peritoneal lavage and the serum, we isolated ILC2s from the mwat of the peritoneal cavity and measured ILC2 cytokine secretion (Fig. 6C). We observed that *N.b.* challenge induced an increase in IL-5^{+} and IL-13^{+} ILC2s in WT animals, but not in *Il33*$^{-/-}$ mice (Fig. 6D–G). Furthermore, eosinophil recruitment to the peritoneal cavity following *N.b.* challenge was dependent on IL-33 (Fig. 6G). Collectively, these data suggest that in addition to influence of ASPC-derived IL-33 on WAT and immune cells, mesothelium-derived IL-33 acts as an alarmin, inducing ILC2 and eosinophil responses upon the breach of the peritoneal barrier.

Discussion

Despite the importance of the IL-33-ST2 pathway in regulating immune cell homeostasis in WAT, the sources of IL-33 have remained elusive. In this report we identify WAT-resident mesenchyme-derived stromal cells as the dominant producers of IL-33. ASPCs produced IL-33 in WAT of visceral and subcutaneous origin, which in turn promoted the production of type 2 cytokines by ILC2s that are known to maintain an anti-inflammatory immune tone. Consistent with this, the loss of IL-33 expression enabled rapid growth of visceral WAT mass and an increase in body weight via elevated ASPC proliferation. Furthermore, IL-33 signaling in WAT suppressed the recruitment of pro-inflammatory immune cells following HFD feeding. We also identify that mesothelial cells that line internal organs, including WAT depots in visceral body cavities, highly expressed nuclear IL-33 that acted as an alarmin by inducing a peritoneal immune response upon infection.

IL-33 is constitutively expressed in a broad range of cell types in most mouse and human tissues, including epithelial cells, endothelial cells and fibroblasts. Highest expression is reported in epithelial cells at mucosal tissue sites, such as the lung and the intestine (16–21). IL-33 tissue levels are increased in inflammatory human diseases such as chronic obstructive

pulmonary disease, asthma, atopic dermatitis and graft versus host disease but also in infectious and inflammatory disease models in mice (27). Although *Il33* transcription can be induced in hematopoietic cells, including macrophages, DCs and mast cells, their capacity to produce IL-33 is considered inferior to structural cells (27, 32).

In addition to epithelial, granulocytic and myeloid cell lineages, several recent studies have characterized IL-33-producing stromal cells that express mesenchymal cell markers and support ILC2 activity in different tissues, including WAT (16, 33–36). For example, Dahlgren et al. recently identified a population of perivascular fibroblast-like stromal cells in the lung that express IL-33 and TSLP and control type 2 immunity (36). A morphologically similar IL-33-producing stromal cell type was also described in the intestine (37). These intestinal pericryptal fibroblasts expressed IL-33 that was regulated by inflammatory stimuli, including TNF-α and IL-1β, and maintained intestinal barrier function following infection (37). A recent study also identified an IL-33-expressing mesenchymal cell in the pericryptal niche of the human colon using unbiased single-cell profiling (38). This intestinal stromal cell responded to inflammatory cues by upregulating *Il33* expression (38). In the context of WAT, cell adhesion molecule cadherin-11 was shown to regulate IL-33 expression in PDGFRα$^+$ stromal cells and promote anti-inflammatory responses (34). Pro-inflammatory cytokines including TNF-α and IL-17A produced by γδ T cells induced PDGFRα$^+$ PDPN$^+$ stromal cell production of IL-33 in WAT (35). Based on these findings, a model emerges whereby IL-33-expressing stromal cells respond to pro-inflammatory stimuli and produce IL-33 that subsequently promotes the anti-inflammatory response and maintains tissue homeostasis. Whether similar pathways are operating in the context of other inflammatory conditions such as asthma, atopic dermatitis or inflammatory bowel disease, is an area worthy of future exploration.

Mesenchyme-derived stem/stromal cells have received much attention for their potential use in tissue engineering and adoptive cellular therapies. We showed that adoptive transfer of ASPCs promoted type 2 immunity in an IL-33-dependent manner. Whether IL-33 contributes to the tissue-remodeling and anti-inflammatory effects of mesenchyme-derived stem/stromal cell therapies remains an intriguing question.

In summary, we find that ASPCs, through their production of IL-33, create an immunological milieu that promotes the activation of ILC2s that in turn play a central role in restricting the activation of the pro-inflammatory arm of the immune system in WAT (8, 13, 39). Our findings, coupled with those of Mathis and colleagues (46), indicate that ASPC-derived IL-33 simultaneously promotes ILC2 and Treg responses in adipose tissue, further highlighting the conserved functions of these tissue-resident cells in the regulation of both innate and adaptive lymphocyte responses. Reciprocally, these immune cells control a vital feedback mechanism and maintain an anti-inflammatory immune environment in adipose depots that sustains normal tissue homeostasis. More broadly, these findings add to a growing awareness of tissue-specific immune regulatory mechanisms and the role of evolutionarily conserved non-hematopoietic progenitor cells in controlling complex immunological and physiological processes in peripheral tissues.

Materials and Methods

Mice

Wild type C57BL/6 mice were purchased from Jackson Laboratories (Bar Harbor, ME) or bred in house. *Il33*$^{-/-}$ mice on a C57BL/6 background were provided by Amgen Inc (Seattle, WA). *Il1rl1*$^{-/-}$ mice backcrossed to C57BL/6 background were generated by Andrew McKenzie and provided by Paul Bryce (Northwestern University). The *Il33*$^{fl/fl}$-*eGFP* mouse (in text termed IL-33-eGFP) was provided by Paul Bryce (Northwestern University) and is available from Jackson Laboratories (Stock No: 030619) (40). *Il33*$^{-/-}$, *Il1rl1*$^{-/-}$ and *IL33*$^{fl/fl}$-*eGFP* mice were bred at Weill Cornell Medicine. All mice used in experiments were age-matched males between 6 and 16 weeks of age. Male mice were used because the effect of female hormones and hormonal cycling on insulin secretion and metabolism are excluded. Also, metabolic phenotypes are more severe in males in many animal models. Animals had *ad libitum* access to standard autoclavable rodent chow (Ctrl, 5% kcal fat, 5010, Lab Diets, St. Louis, Missouri) and water and were maintained in a specific-pathogen free facility with a 12 h : 12 h light:dark cycle. Where indicated, mice were fed a high fat diet (HFD, 60% kcal fat, Research Diets) for the indicated period. Animals were randomly assigned to groups of n=3–5 mice per group per experiment, and at least two independent experiments were performed throughout. No animals were excluded from the analysis. All animal experiments were approved and are in accordance with the local animal care committees.

Cell isolation

Murine epididymal WAT (ewat), mesentery or subcutaneous (inguinal) WAT (iwat) were harvested and digested in 1mg/ml collagenase type II (Collagenase from *Clostridium histolyticum*, SIGMA, C6885–5G) in DMEM (GIBCO) at 37°C with shaking at 200 rpm. for 30–45 min. Digested tissues were filtered through a 70-μm nylon mesh and centrifuged at 600g for 10 min. Floating adipocytes were removed, and the stromal vascular fraction (SVF) pellet was resuspended in red blood cell lysis buffer (ACK RBC Lysis Buffer, Lonza). Recovered cells were washed with cold 2%Fetal Bovine Serum (FBS, Omega Scientific) in PBS and stained with live/dead stain (Molecular Probes) followed by standard surface staining for flow cytometric analysis with fluorochrome-conjugated antibodies.

Flow cytometry and cell sorting

After blocking the Fc-receptors with CD16/CD32 antibody (Biolegend), cell suspensions of murine WAT were incubated on ice with fluorochrome-conjugated antibodies in PBS. The following antibodies were used to stain cells from mouse tissues: CD3ε (145–2C11), CD5 (53–7.3), FcεRI (Mar-1), B220 (RA3–6B2), CD11b (M1/70), CD11c (N418), NK1.1 (PK136), KLRG1 (2F1), CD45 (30-F11), CD45.2 (104), CD25 (PC61), CD127 (A7R34), SiglecF (E50–2440), CD90.2 (53–2.1), ST2 (DIH9), GATA3 (TWAJ), F4/80 (BM8), CD64 (X54–5/7.1), CD140a (APA5), CD140b (APB5), CD49a (Ha31/8), CD51 (RMV-7), CD29 (HMβ1–1), CD73 (TY/11.8), Ter119 (TER-119), CD31 (390), CD34 (RAM34), PDPN (eBio8.1.1), Sca-1 (D7), CD24 (M1/69), MSLN (295D) (MBL), Ly6C (HK1.4) and CD9 (KMC8). GATA-3 (TWAJ), IL-33 (Polyclonal Goat anti mouse; R&D Systems) and Ki67 (B56) were stained using the Foxp3 transcription factor staining buffer set (eBioscience). All

antibodies used in flow cytometry were purchased from eBioscience, Biolegend or BD Biosciences if not indicated above otherwise. Cells from human tissues were stained with antibodies to IL-33 (IC3625P) from R&D Systems, CD34 (4H11) from eBioscience, PDGFRα (16A1) and CD31 (WM59) from Biolegend and CD45 (HI30) from BD Biosciences. All flow cytometry experiments were acquired using Fortessa flow cytometer and cells sort-purified using FACSAria cell sorter (BD Biosciences). Data were analyzed with FlowJo V10.4.1 software (TreeStar).

Intracellular cytokine analysis

To examine cytokine production in ILC2s, single-cell suspensions of SVF were cultured for 4h *ex vivo* with phorbol 12-myristate 13-acetate (PMA) (Sigma-Aldrich) (100 ng/ml) and ionomycin (Sigma-Aldrich) (1 μg/ml) in the presence of brefeldinA (10 μg/ml) (Sigma-Aldrich) in a 37°C incubator (5% CO2). Cells were washed with cold PBS and surface stained before fixation and permeabilization using the Cytofix/Cytoperm Fixation/ Permeabilization Solution and Perm/Wash buffer according to the manufacturer's protocol (BD Biosciences). Intracellular staining was performed with IL-5 (TRFK5) and IL-13 (eBIO13A) antibodies (eBioscience).

Adoptive cell transfer

5×10^4 FACS-sorted live $CD31^-$ $Ter119^-$ $CD45^-$ $PDGFR\alpha^+$ donor ASPCs from $Il33^{-/-}$ or wild type animals were injected intraperitoneally into $Il33^{-/-}$ hosts. WAT from mice were analyzed 6 weeks after adoptive transfer.

Quantitative real-time PCR

Adipose tissues were snap-frozen in Trizol (Thermo Fisher Scientific) and homogenized using Tissue Lyser (Qiagen). RNA was isolated using the RNeasy kit (Qiagen) following the manufacturer's instructions. Sorted cells were homogenized in Trizol (Thermo Fisher Scientific) and RNA extracted according to manufacturer's protocol. Reverse transcription of total RNA was performed using the High Capacity cDNA Reverse Transcription kit according to the manufacturer's protocol (Thermo Fisher Scientific). Reaction was run on a QuantStudio 6 Flex Real-Time PCR (Thermo Fisher Scientific) using the following TaqMan Gene Expression Assays (Applied Biosystems): Gene expression was normalized to the housekeeping gene *Hprt1* (Mm00446968_m1). Calculation of mRNA levels was performed with the QuantStudio Real-Time PCR software version 1.0 (Thermo Fisher Scientific). Primer sets used: *Cd3* (QT01058764), *Ccl11* (QT00114275), *Il33* (QT00135170), *Il33* F 5'-GCTGCGTCTGTTGACACATT-3', *Il33* R 5'-CACCTGGTCTTGCTCTTGGT-3', *Mcp1* F 5'-GTTGGCTCAGCCAGATGCA-3', *Mcp1* R 5'-AGCCTACTCATTGGGATCATCTTG-3', *Pdgfra* F 5'-AGCAGGCAGGGCTTCAACGG-3', *Pdgfra* R 5'-ACACAGTCTGGCGTGCGTCC-3', *Msln* F 5'-ACCTGAAGACCGAGGAGGAT-3', Msln R 5'-AAGTCCAGGACCAGGTAGCC-3', *Adiponectin* F 5'-GGAGAGAAAGGAGATGCAGT-3', *Adiponectin* R 5'-CTTTCCTGCCAGGGGTTC-3', *Lrrn4* F 5'-TGAGTTCCTTTGGTCCTTGG-3', *Lrrn4* R 5'-TGTTGACATCCACGAGAAGC-3', *Upk3b* F 5'-AATCCCAACTCCATTGACACA-3', *Upk3b* R 5'-TAGTGGAAGCTGCCAGGAAA-3'.

Cell culture and cytokine measurements

Sort-purified ASPCs were cultured in high glucose DMEM supplemented with 10% FBS, 100 U/ml Penicillin and 100 μg/ml Streptomycin (all from Gibco) in 12-well plates (Corning) until confluency and supernatant collected for ILC2 stimulation. Cytokines in ASPC supernatants were analyzed by Eve Technologies. 10^4 sort-purified ILC2s were cultured in ASPC-conditioned medium in 96-well microtiter plates for 24h at 37°C and 5% CO2. Cytokines in the supernatant were detected with a sandwich ELISA using IL-5 (TRFK5) or IL-13 (eBio13a) as capture antibodies and IL-5 (TRFK4) or IL-13 (eBio1316H) as detection antibodies (eBioscience) or the Legendplex bead-based assay (Biolegend) for IL-5 and IL-13 according to the manufacturer's protocol.

RNAseq analysis

ASPCs were sort-purified from visceral adipose tissue (epididymal WAT) of wild type C57BL/6 mice. Sorted cells were used to prepare RNAseq libraries by the Epigenomics Core at Weill Cornell Medicine using the Clontech SMARTer® Ultra® Low Input RNA Kit V4 (Clontech Laboratories). Sequencing was performed on an Illumina HiSeq 2500, yielding 50 bp single end reads. Raw sequencing reads were demultiplexed with Illumina's CASAVA (v1.8.2). Adapters were trimmed from reads using FLEXBAR (v2.4) (41) and reads were aligned to the NCBI GRCm38/mm10 mouse genome using the STAR aligner (v2.3.0) (42) with default settings. Reads per gene were counted using Rsubread (43). Normalized counts per gene were calculated using using DESeq2 version 1.18.1 (44).

Immunofluorescence

Adipose tissue was excised and fixed in 2% paraformaldehyde (PFA)(Electron Microscopy Sciences) for 2h on ice for whole mount tissue staining or in 4% PFA overnight on ice for paraffin embedding and sectioning. For whole mount staining, tissue was washed in ice-cold PBS and blocked with 10% donkey serum in 0.1% Triton X-100 and PBS, and stained with indicated antibodies. The following antibodies were used: polyclonal goat anti-mPDGFRα AF1062 (R&D Systems), rabbit anti-perilipin (D1D8) (Cell Signaling Technologies), rat anti-CD45 (30-F11) and rat anti-ZO-1 IgG2a (R26.4C), PE- or APC-conjugated Syrian hamster anti-PDPN IgG (eBio8.1.1) and PE- or APC-conjugated rat anti-CD140a (PDGFRα) IgG2a (APA5), APC-conjugated anti-CD3ε (145–2C11), PE-conjugated anti-KLRG1 (2F1) from Invitrogen via Thermo Fisher Scientific or rabbit anti-Wilms tumor protein antibody (CAN-R9(IHC)-56–2) (Abcam), polyclonal goat anti-mouse IL-33 (R&D Systems). If needed, primary antibodies were followed by secondary conjugated antibodies: donkey anti-rat IgG Alexa Fluor (AF) 488, goat anti-rabbit IgG AF405, goat anti-rabbit IgG AF488, goat anti-rabbit IgG AF647, donkey anti-rabbit IgG AF647, goat anti-rat IgG AF555, goat anti-rabbit IgG AF488, goat anti-rat IgG AF555, all from Invitrogen via Thermo Fisher Scientific, or donkey anti-goat IgG AF594, donkey anti-goat IgG AF647, donkey anti-goat IgG AF488 (Jackson Immune Research). Adipose tissue from the IL-33-eGFP reporter mouse was imaged fresh as a sharp decrease in eGFP signal was seen upon tissue manipulation or fixation. Sections of paraffin embedded human tissues were stained with mouse anti-human IL-33 (Nessy-1) (Enzo), Rabbit anti-perilipin (D1D8) (Cell

Signaling Technologies). Representative images were captured using a Nikon Eclipse Ti microscope and NIS-Elements 4.30.02 software (Nikon).

High-fat diet

Where indicated, mice were fed a high fat diet (HFD, 60% kcal fat, Research Diets) for 3 to 7 days starting at 6–8 weeks of age. HFD was gamma-irradiated (10–20 kGy). Standard chow was used as control diet (CD).

Nippostrongylus brasiliensis (N.b.)* infection—N. b.* life cycle was maintained as described previously (45). Mice were infected intraperitoneally with 500 L3 larvae and analyses were preformed at 1 hour or 4 hours post infection.

Recombinant murine IL-33 treatment

Mice were treated intraperitoneally with carrier-free recombinant murine IL-33 (12.5μg/kg body weight; R&D) in sterile PBS on 3 days and 1 day before analysis.

Statistical analysis

P value of data sets was determined by unpaired two-tailed Student's t-test with 95% confidence interval. Normal distribution was assumed. All statistical tests were performed with Graph Pad Prism V6 software. (*$p < 0.05$, **$p < 0.01$, ***$p < 0.001$; **** $p < 0.0001$, ns -, not significant). Investigators were not blinded to group allocation during experiments.

Supplementary Material

Refer to Web version on PubMed Central for supplementary material.

Acknowledgments:

We thank the Artis lab members for discussion and critical reading of the manuscript. We thank the epigenomics core at Weill Cornell Medicine for carrying out RNA sequencing.

Funding: This work was supported by grants from the Crohn's & Colitis Foundation (to T.M. and D.A.), the Jill Roberts Institute (to G.G.P. and D.A.), Cure for IBD (to D.A.), the Burroughs Wellcome Fund (to D.A.), the Rosanne H. Silbermann Foundation (to D.A.) and the NIH (AI105839 (to P.B.), AI074878, AI095466, AI095608, AI102942, AI106697 (to D.A.) and the NIAID Mucosal Immunology Studies Team (MIST) (to D.A.)).

References and Notes:

1. Hales CM, Carroll MD, Fryar CD, Ogden CL, Prevalence of Obesity Among Adults and Youth: United States, 2015–2016. NCHS Data Brief, 1–8 (2017).
2. Gonzalez-Muniesa P et al., Obesity. Nat Rev Dis Primers 3, 17034 (2017).
3. Brestoff JR, Artis D, Immune regulation of metabolic homeostasis in health and disease. Cell 161, 146–160 (2015). [PubMed: 25815992]
4. Melen E et al., Analyses of shared genetic factors between asthma and obesity in children. J Allergy Clin Immunol 126, 631–637 e631–638 (2010). [PubMed: 20816195]
5. Angeles-Martinez J et al., The rs7044343 Polymorphism of the Interleukin 33 Gene Is Associated with Decreased Risk of Developing Premature Coronary Artery Disease and Central Obesity, and Could Be Involved in Regulating the Production of IL-33. PLoS One 12, e0168828 (2017).

6. Hasan A et al., IL-33 is negatively associated with the BMI and confers a protective lipid/metabolic profile in non-diabetic but not diabetic subjects. BMC Immunol 15, 19 (2014). [PubMed: 24886535]
7. Brestoff JR et al., Group 2 innate lymphoid cells promote beiging of white adipose tissue and limit obesity. Nature 519, 242–246 (2015). [PubMed: 25533952]
8. Lee MW et al., Activated type 2 innate lymphoid cells regulate beige fat biogenesis. Cell 160, 74–87 (2015). [PubMed: 25543153]
9. Cautivo KM, Molofsky AB, Regulation of metabolic health and adipose tissue function by group 2 innate lymphoid cells. Eur J Immunol 46, 1315–1325 (2016). [PubMed: 27120716]
10. Duffen J et al., Modulation of the IL-33/IL-13 Axis in Obesity by IL-13Ralpha2. J Immunol 200, 1347–1359 (2018). [PubMed: 29305434]
11. Han JM et al., IL-33 Reverses an Obesity-Induced Deficit in Visceral Adipose Tissue ST2+ T Regulatory Cells and Ameliorates Adipose Tissue Inflammation and Insulin Resistance. J Immunol 194, 4777–4783 (2015). [PubMed: 25870243]
12. Miller AM et al., Interleukin-33 induces protective effects in adipose tissue inflammation during obesity in mice. Circ Res 107, 650–658 (2010). [PubMed: 20634488]
13. Molofsky AB et al., Innate lymphoid type 2 cells sustain visceral adipose tissue eosinophils and alternatively activated macrophages. J Exp Med 210, 535–549 (2013). [PubMed: 23420878]
14. Moro K et al., Innate production of T(H)2 cytokines by adipose tissue-associated c-Kit(+)Sca-1(+) lymphoid cells. Nature 463, 540–544 (2010). [PubMed: 20023630]
15. Vasanthakumar A et al., The transcriptional regulators IRF4, BATF and IL-33 orchestrate development and maintenance of adipose tissue-resident regulatory T cells. Nat Immunol 16, 276–285 (2015). [PubMed: 25599561]
16. Kolodin D et al., Antigen- and cytokine-driven accumulation of regulatory T cells in visceral adipose tissue of lean mice. Cell Metab 21, 543–557 (2015). [PubMed: 25863247]
17. Molofsky AB, Savage AK, Locksley RM, Interleukin-33 in Tissue Homeostasis, Injury, and Inflammation. Immunity 42, 1005–1019 (2015). [PubMed: 26084021]
18. Moussion C, Ortega N, Girard JP, The IL-1-like cytokine IL-33 is constitutively expressed in the nucleus of endothelial cells and epithelial cells in vivo: a novel ‘alarmin’? PLoS One 3, e3331 (2008).
19. Pichery M et al., Endogenous IL-33 is highly expressed in mouse epithelial barrier tissues, lymphoid organs, brain, embryos, and inflamed tissues: in situ analysis using a novel Il-33-LacZ gene trap reporter strain. J Immunol 188, 3488–3495 (2012). [PubMed: 22371395]
20. Wood IS, Wang B, Trayhurn P, IL-33, a recently identified interleukin-1 gene family member, is expressed in human adipocytes. Biochem Biophys Res Commun 384, 105–109 (2009). [PubMed: 19393621]
21. Zeyda M et al., Severe obesity increases adipose tissue expression of interleukin-33 and its receptor ST2, both predominantly detectable in endothelial cells of human adipose tissue. Int J Obes (Lond) 37, 658–665 (2013). [PubMed: 22828942]
22. Hsu CL, Neilsen CV, Bryce PJ, IL-33 is produced by mast cells and regulates IgE-dependent inflammation. PLoS One 5, e11944 (2010).
23. Talabot-Ayer D et al., The mouse interleukin (Il)33 gene is expressed in a cell type- and stimulus-dependent manner from two alternative promoters. J Leukoc Biol 91, 119–125 (2012). [PubMed: 22013230]
24. Hepler C et al., Identification of functionally distinct fibro-inflammatory and adipogenic stromal subpopulations in visceral adipose tissue of adult mice. Elife 7, (2018).
25. Gupta OT, Gupta RK, Visceral Adipose Tissue Mesothelial Cells: Living on the Edge or Just Taking Up Space? Trends Endocrinol Metab 26, 515–523 (2015). [PubMed: 26412153]
26. Chau YY et al., Visceral and subcutaneous fat have different origins and evidence supports a mesothelial source. Nat Cell Biol 16, 367–375 (2014). [PubMed: 24609269]
27. Liew FY, Girard JP, Turnquist HR, Interleukin-33 in health and disease. Nat Rev Immunol 16, 676–689 (2016). [PubMed: 27640624]

28. Jeffery E, Church CD, Holtrup B, Colman L, Rodeheffer MS, Rapid depot-specific activation of adipocyte precursor cells at the onset of obesity. Nat Cell Biol 17, 376–385 (2015). [PubMed: 25730471]
29. Berry R, Rodeheffer MS, Characterization of the adipocyte cellular lineage in vivo. Nat Cell Biol 15, 302–308 (2013). [PubMed: 23434825]
30. Rodeheffer MS, Birsoy K, Friedman JM, Identification of white adipocyte progenitor cells in vivo. Cell 135, 240–249 (2008). [PubMed: 18835024]
31. Hung LY et al., IL-33 drives biphasic IL-13 production for noncanonical Type 2 immunity against hookworms. Proc Natl Acad Sci U S A 110, 282–287 (2013). [PubMed: 23248269]
32. Schmitz J et al., IL-33, an interleukin-1-like cytokine that signals via the IL-1 receptor-related protein ST2 and induces T helper type 2-associated cytokines. Immunity 23, 479–490 (2005). [PubMed: 16286016]
33. Koga S et al., Peripheral PDGFRα. J Exp Med 215, 1609–1626 (2018). [PubMed: 29728440]
34. Chang SK et al., Stromal cell cadherin-11 regulates adipose tissue inflammation and diabetes. J Clin Invest 127, 3300–3312 (2017). [PubMed: 28758901]
35. Kohlgruber AC et al., γδ T cells producing interleukin-17A regulate adipose regulatory T cell homeostasis and thermogenesis. Nat Immunol 19, 464–474 (2018). [PubMed: 29670241]
36. Dahlgren MW et al., Adventitial Stromal Cells Define Group 2 Innate Lymphoid Cell Tissue Niches. Immunity 50, 707–722.e706 (2019).
37. Mahapatro M et al., Programming of Intestinal Epithelial Differentiation by IL-33 Derived from Pericryptal Fibroblasts in Response to Systemic Infection. Cell Rep 15, 1743–1756 (2016). [PubMed: 27184849]
38. Kinchen J et al., Structural Remodeling of the Human Colonic Mesenchyme in Inflammatory Bowel Disease. Cell 175, 372–386.e317 (2018).
39. Zhang Y et al., Eosinophils Reduce Chronic Inflammation in Adipose Tissue by Secreting Th2 Cytokines and Promoting M2 Macrophages Polarization. Int J Endocrinol 2015, 565760 (2015).
40. Han H et al., IL-33 promotes gastrointestinal allergy in a TSLP-independent manner. Mucosal Immunol 11, 578 (2018). [PubMed: 29067997]
41. Dodt M, Roehr JT, Ahmed R, Dieterich C, FLEXBAR-Flexible Barcode and Adapter Processing for Next-Generation Sequencing Platforms. Biology (Basel) 1, 895–905 (2012). [PubMed: 24832523]
42. Dobin A et al., STAR: ultrafast universal RNA-seq aligner. Bioinformatics 29, 15–21 (2013). [PubMed: 23104886]
43. Liao Y, Smyth GK, Shi W, The Subread aligner: fast, accurate and scalable read mapping by seed-and-vote. Nucleic Acids Res 41, e108 (2013).
44. Love MI, Huber W, Anders S, Moderated estimation of fold change and dispersion for RNA-seq data with DESeq2. Genome Biol 15, 550 (2014). [PubMed: 25516281]
45. Camberis M, Le Gros G, Urban J Jr., Animal model of Nippostrongylus brasiliensis and Heligmosomoides polygyrus. Curr Protoc Immunol Chapter 19, Unit 19 12 (2003).
46. Spallanzani RG et al., Distinct immunocyte-promoting and adipocyte-generating stromal components coordinate adipose-tissue immune and metabolic tenors. Sci. Immunol 4, eaaw3658 (2019).

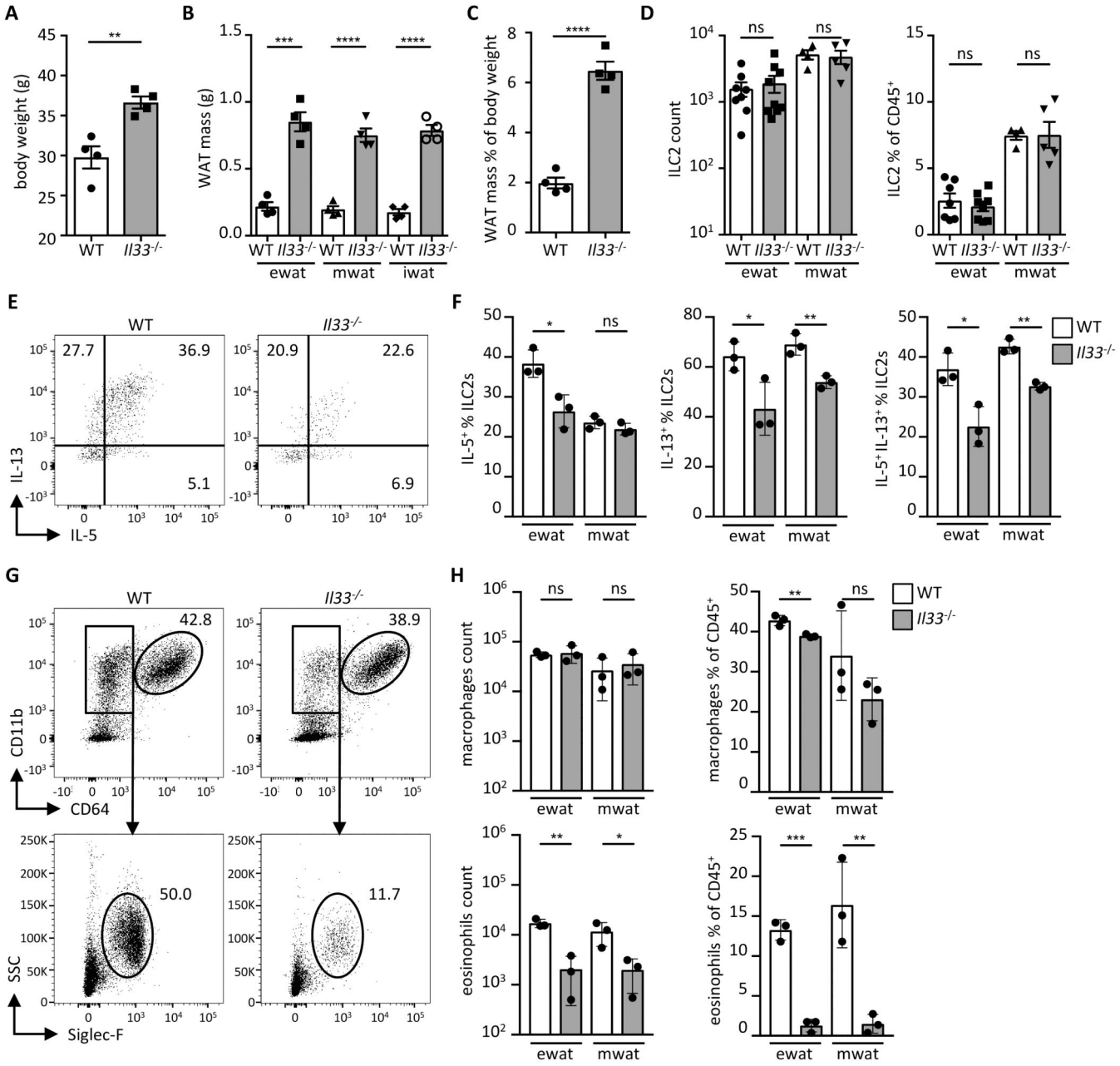

Fig. 1.

IL-33 regulates ILC2 activity and eosinophil numbers. (**A**) Body weight of wild type (WT) and *Il33*$^{-/-}$ mice on conventional diet at 16 weeks of age. (n = 4) (**B**) Mass of indicated adipose depots in WT and *Il33*$^{-/-}$ mice at 16 weeks of age. (n = 4) (**C**) Proportion of combined white adipose tissue (WAT) mass of epididymal (ewat), mesenteric (mwat) and inguinal (iwat) depots as percent of body weight in WT and *Il33*$^{-/-}$ mice at 16 weeks of age. (n = 4) (**D**) ILC2 numbers and proportions in visceral adipose compartments of WT and *Il33*$^{-/-}$ mice. (n ≥ 3) Data pooled from two individual experiments. (**E** and **F**) Representative dot plots (**E**) and quantification (**F**) showing intracellular IL-5 and IL-13 staining in ILC2s from visceral adipose depots of WT and *Il33*$^{-/-}$ mice. (n = 3) (**G** and **H**) Representative dot

plots (**G**) and quantification (**H**) of macrophages and eosinophils in visceral adipose depots of WT and *Il33*$^{-/-}$ mice. (n = 3). Mean ± SEM, * $P < 0.05$, ** $P < 0.01$, *** $P < 0.001$, ns - not significant, Student's *t*-test.

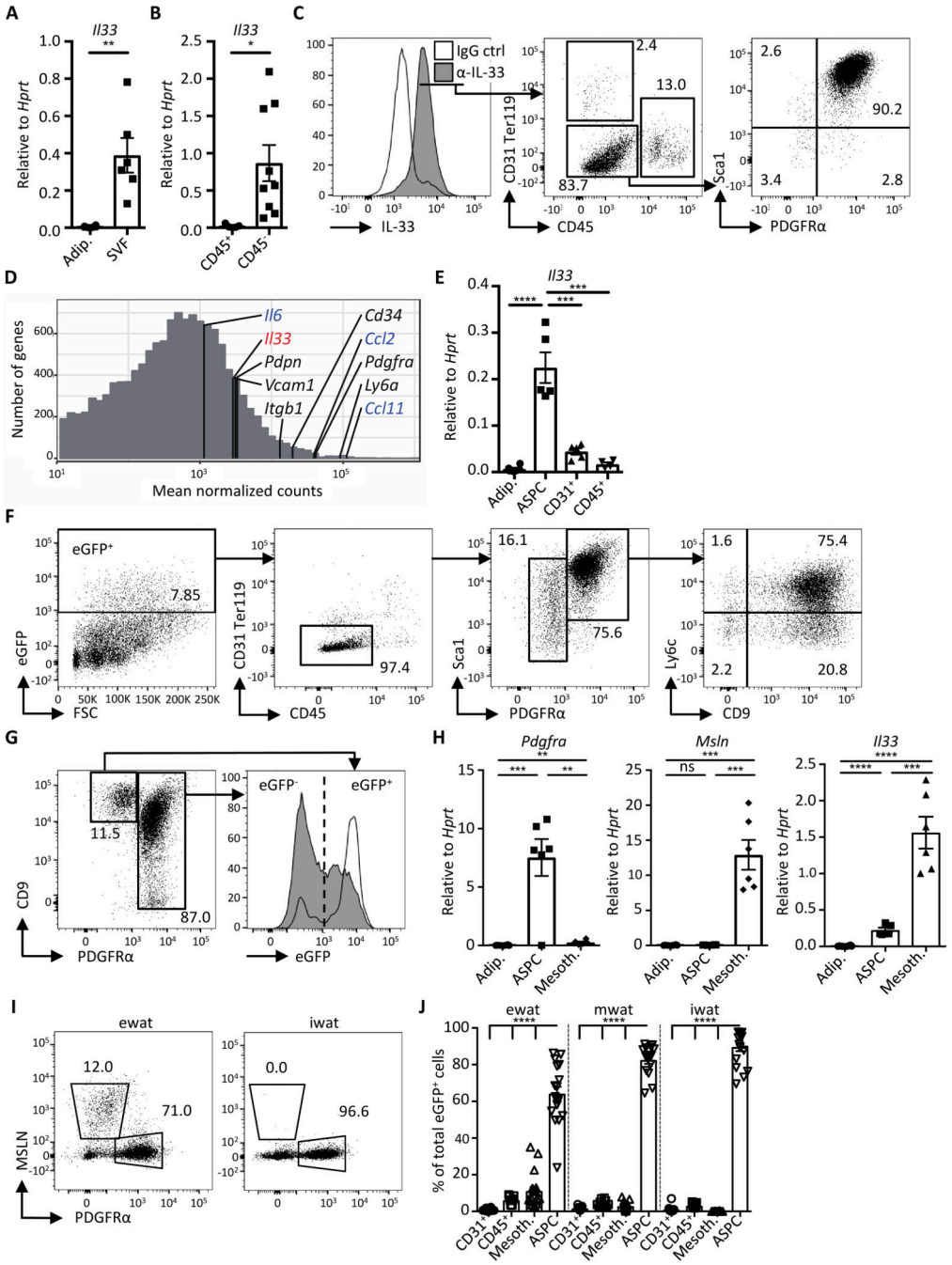

Fig. 2.

Visceral WAT adipose stem and progenitor cells produce IL-33. (**A** and **B**) Expression of *Il33* in (**A**) isolated adipocytes (adip.), stromal vascular fraction (SVF) and in (**B**) indicated sort-purified cells of murine epididymal WAT (ewat) as determined by qRT-PCR analysis. ($n \geq 5$) (**C**) Representative histogram overlay and dot plots of cells in ewat SVF fraction of wild type mice, stained with anti-IL-33 (α-IL-33) and IgG control (ctrl) antibodies. Data depicted are gated on live cells. Numbers in gates indicate proportion (%) of parent gate. (**D**) Histogram demonstrating mean normalized counts from RNAseq of genes expressed in sort-

purified ASPCs from ewat. Markers of ASPCs are indicated in black, highly expressed cytokine genes are indicated in blue, and *Il33* is shown in red. Genes with mean normalized counts < 10 are not shown. (n = 3) (**E**) Expression of *Il33* in adipocytes and sort-purified cells from ewat as determined by qRT-PCR analysis. (n ≥ 5) (**F**) Representative dot plots showing eGFP-expressing cells in ewat of the IL-33-eGFP mouse. Numbers in gates indicate proportion (%) of parent gate. Data shown are gated on live cells. (**G**) Representative dot plot and histogram overlay of live $eGFP^+$ lin^- ($CD31^+$ $CD45^+$ $Ter119^+$) cells in the ewat of the IL-33-eGFP mouse. (**H**) Expression of indicated genes in isolated adipocytes and sort-purified cells from the ewat as determined by qRT-PCR analysis. (n ≥ 5) (**I**) Representative dot plots of mesothelin (MSLN) staining in wild type mouse SVF from ewat and subcutaneous WAT (inguinal WAT; iwat) first gated on live lin^- cells. Numbers in gates indicate proportion (%) of the parent gate. (**J**) Quantification of $eGFP^+$ cell populations in indicated WAT compartments. Data were compiled from three independent experiments (n ≥ 13). Mean ± SEM, * $P < 0.05$, ** $P < 0.01$, *** $P < 0.001$, **** $P < 0.0001$, ns - not significant, Student's *t*-test.

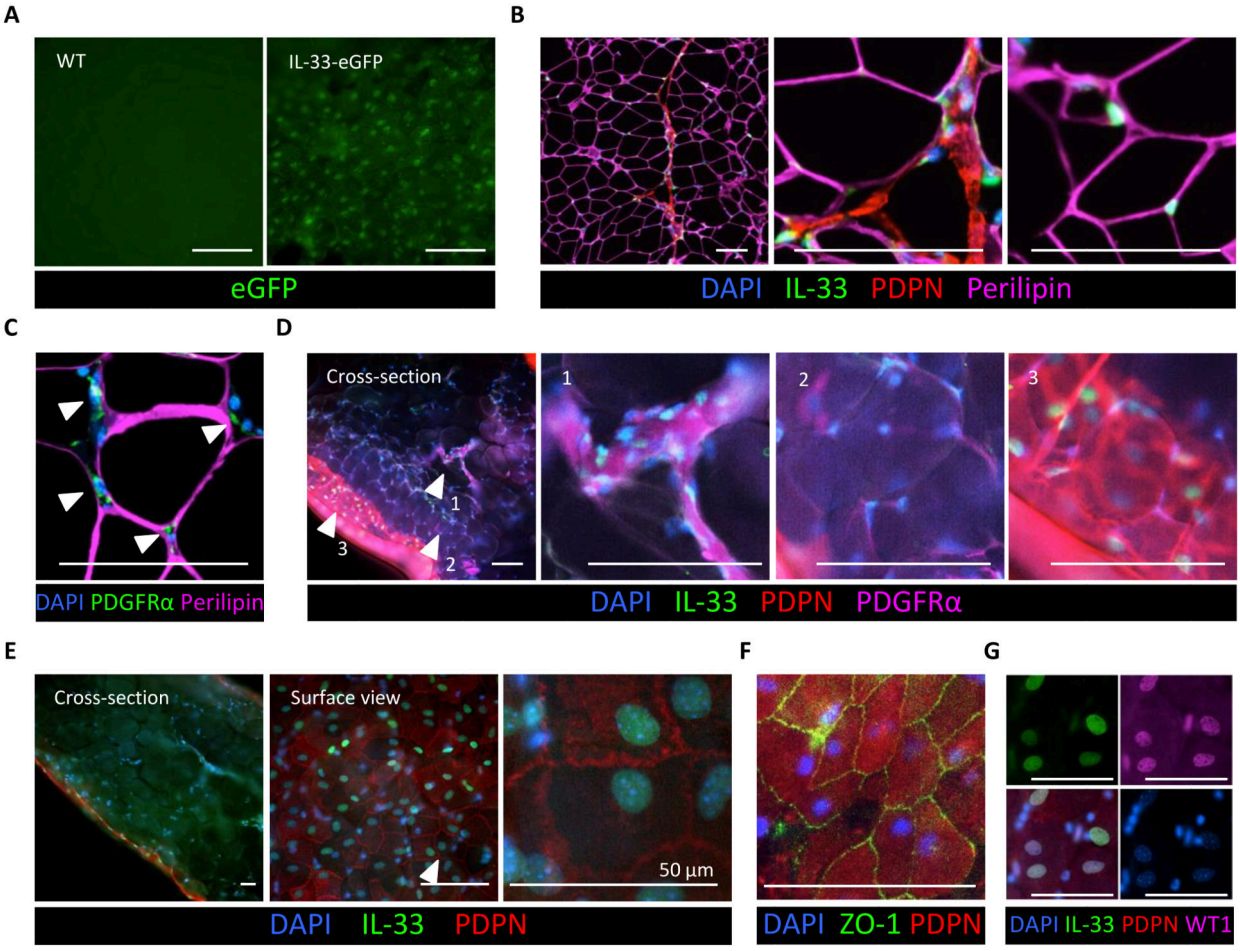

Fig. 3.

Localization of IL-33-expressing cells in visceral WAT. (**A**) Surface view of the ewat from the IL-33-eGFP reporter mouse (*right*) and a wild type (WT) control animal (*left*). (**B**) Immunostaining of IL-33 (green) in paraffin-embedded WT mouse ewat. Note IL-33 localization to DAPI-stained nuclei (blue) scattered between perilipin^{+} adipocytes (purple), as well as IL-33 in the PDPN^{+} (red) membrane lining the adipose compartment. (**C**) Immunostaining of paraffin-embedded WT mouse ewat. PDGFRα-expressing ASPCs (green) embedded between perilipin^{+} adipocytes (purple). (**D**) Immunostained transverse sections (side view) of whole-mount WT mouse ewat demonstrating PDGFRα-stained (purple) ASPCs that express IL-33 (green) in the nucleus (blue). The PDPN-stained (red) cell layer expressing nuclear IL-33 (green) envelops the adipose compartment. Arrowheads indicate magnified areas in adjacent panels. (**E**) Side and surface view of the same sample of WT mouse whole-mount stained ewat. (**F** and **G**) Surface view of whole-mount stained ewat. ZO1 (green) staining on PDPN^{+} (red) cobblestone-shaped cells in (**F**) and co-localization of IL-33 (green) and WT1 (purple) in the nucleus (blue) in (**G**). Scale bar, 100 µm, unless indicated otherwise. All immunostaining experiments are representative of two mice, and the staining protocol has been repeated minimum of three times.

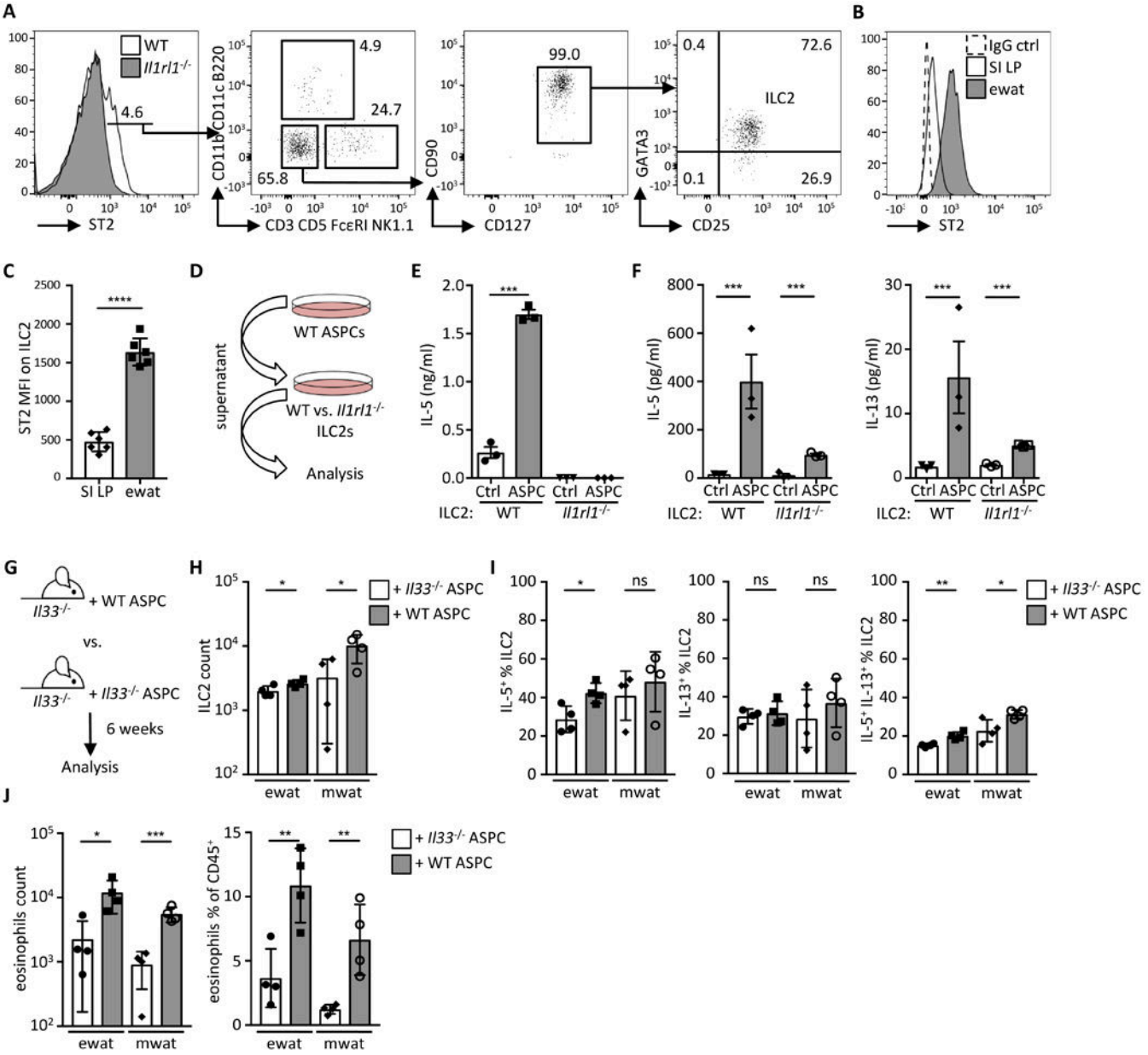

Fig. 4.

Adipose stem and progenitor cell-derived IL-33 controls ILC2 activity. (**A**) Representative histogram and dot plots showing ST2$^+$ cells in the lymphocyte population first gated on live CD45$^+$ cells. (**B**) Representative histogram of ST2 expression on ILC2 (defined as shown in fig. S9A) from the small intestinal lamina propria (SI LP) and epididymal WAT (ewat). (**B** and **C)** Representative histogram (**B**) and bar graph (**C**) showing mean fluorescence intensity (MFI) of ST2 on ILC2s from ewat and SI LP. (n = 6) (**D**) Schematic indicating experimental design for E and F. (**E**) Sort-purified ILC2s from wild type (WT) or *Il1rl1*$^{-/-}$ mouse visceral WAT (pooled ewat and mwat) ILC2s were cultured in ASPC-conditioned (ASPC) or control media (Ctrl) and IL-5 secretion was analyzed by ELISA after 48 h. (n = 3) (**F)** Sort-purified ILC2s from visceral WAT or SI LP were cultured in ASPC-conditioned or control media

(Ctrl) and IL-5 and IL-13 secretion was analyzed by multiplex bead-based assay after 48 h. (n = 3) (**G**) Schematic indicating experimental design. Sort-purified ASPCs from wild type (WT) or *Il33*$^{-/-}$ mice were injected into the peritoneum of *Il33*$^{-/-}$ mice and immunological analysis (**H**-**J**) performed after six weeks in visceral adipose compartments. **(H)** ILC2 numbers, (**I**) proportions of IL-5^{+} and IL-13^{+} ILC2s, and (**J**) eosinophil quantification. (n = 4). Mean ± SEM, * $P < 0.05$, ** $P < 0.01$, *** $P < 0.001$, ns – not significant, Student's *t*-test.

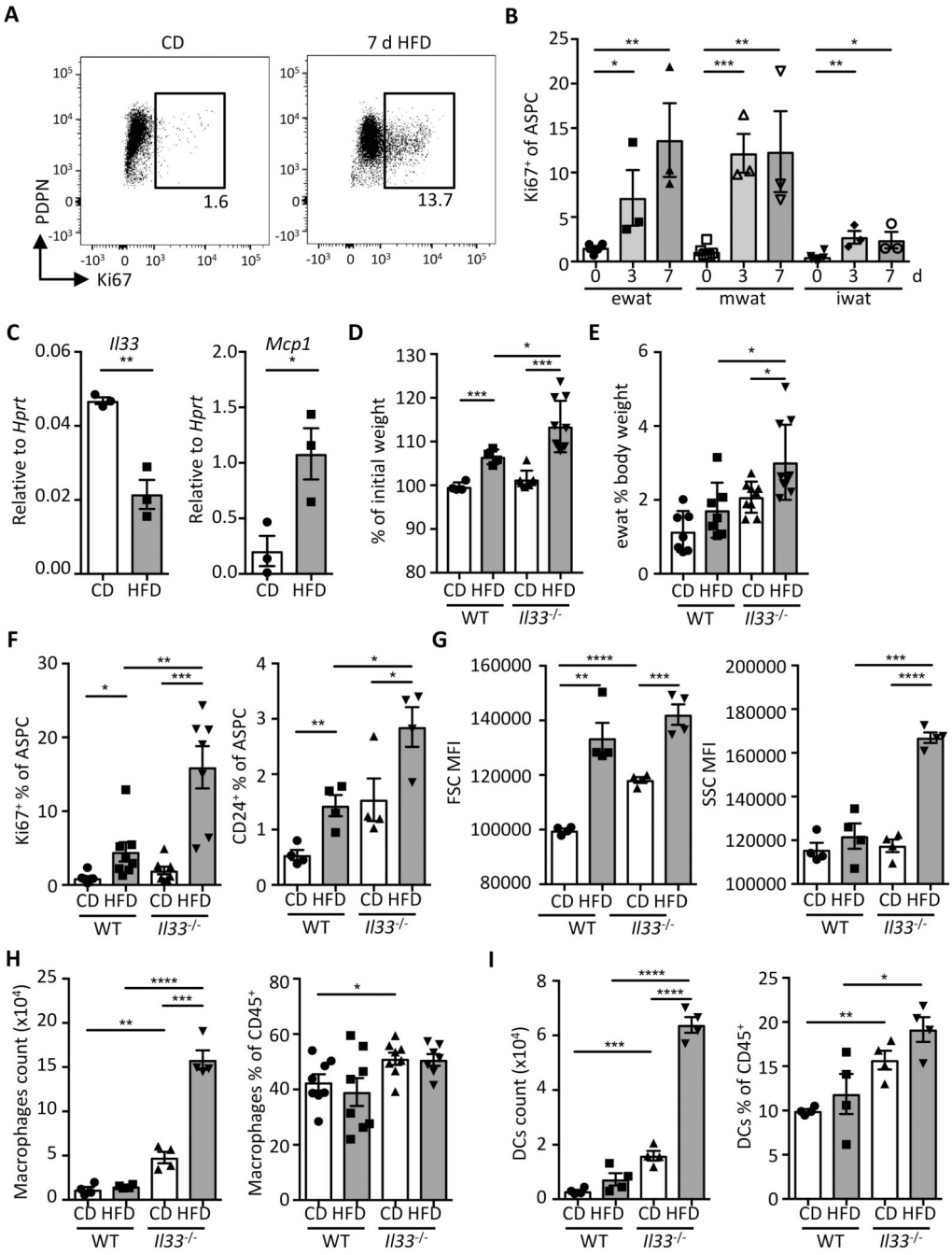

Fig. 5.

IL-33 controls adipose tissue expansion and immunological homeostasis in short-term HFD feeding. (**A**-**B**) Wild type mice were fed with high-fat diet (HFD) or control diet (CD) up to 7 days (d). (**A**) Representative dot plot of Ki67 staining in ASPCs (defined as live lin^{-} (CD31^{-} CD45^{-} Ter119^{-})) PDGFRα^{+}Sca-1^{+} cells) on day 7. (**B**) Proportion of proliferating cells (Ki67^{+}) cells among total ASPCs from indicated WAT depots. (n = 3) (**C**) Expression of *Il33* and *Mcp1* in sort-purified ASPCs isolated from ewat of wild type mice (WT) on CD or HFD for 3 days as determined by qRT-PCR. (n = 3) (**D** to **I**) WT or *Il33*$^{-/-}$ mice were fed

with CD or HFD and sacrificed for analysis after 3 days. (**D**) Body weight change as a proportion (%) of initial weight (day 0). Data compiled from two individual experiments. (n ≥ 7) (**E**) Proportion of ewat mass as proportion (%) of body weight. Data compiled from two individual experiments. (n ≥ 7) (**F**) Proportion of $Ki67^+$ and adipocyte progenitor cells ($CD24^+$) among total ewat ASPCs. (**G**) Mean fluorescence intensity (MFI) of forward scatter (FSC) and side scatter (SSC) of ewat ASPCs. (**H** and **I**) Quantification of macrophages (**H**) and dendritic cells (DCs) (**I**) in ewat. (n ≥ 4). Mean ± SEM, * $P < 0.05$, ** $P < 0.01$, *** $P < 0.001$, Student's *t*-test.

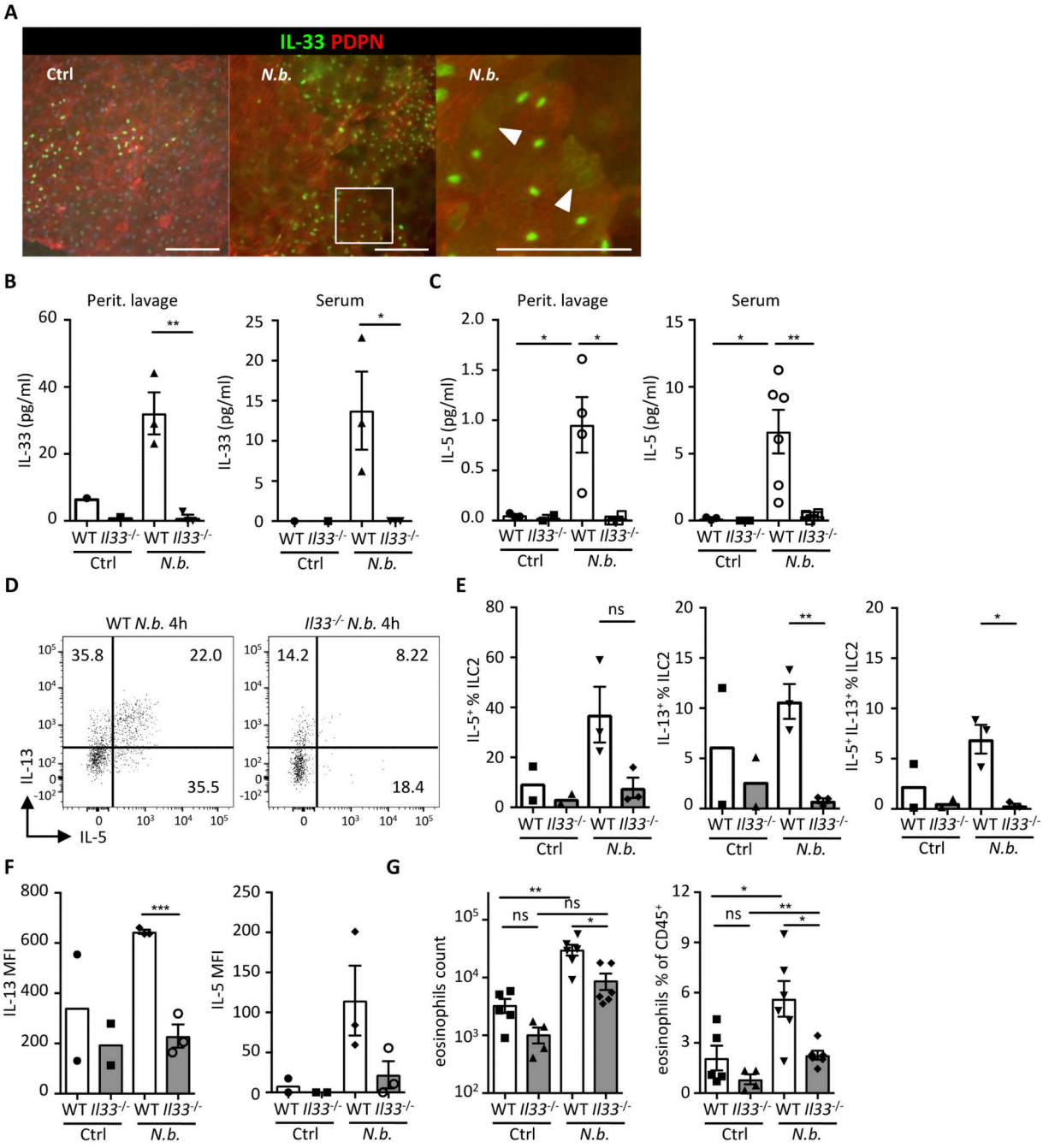

Fig. 6.

Mesothelial IL-33 acts as an alarmin to activate the immune system upon peritoneal infection. (**A**) Wild type (WT) mice were injected i.p. with *Nippostrongylus brasiliensis* (*N.b.*) L3 larvae and epididymal WAT (ewat) extracted after 1 h. Representative surface view of immunostained whole-mount ewat depicting IL-33 (green) and PDPN^{+} mesothelium (red). Note IL-33 relocalization from the nucleus to the cytoplasm in *N.b.*-treated condition. Encircled area indicates magnified area. Arrowheads point to diffuse IL-33 staining in the cytoplasm. (**B** and **C**) ELISA quantification of IL-33 and IL-5 in peritoneal lavage fluid and

serum of wild type (WT) and *Il33*$^{-/-}$ mice 4 h after *N.b.* infection. (n ≥ 3) (**D - E**) Representative dot plots (**D**) and quantification (**E**) showing intracellular IL-5 and IL-13 staining in ILC2s from ewat of WT and *Il33*$^{-/-}$ mice treated with *N.b.* (n ≥ 2) (**F**) Mean fluorescence intensity (MFI) of IL-13 and IL-5 in ILC2s from panels D and E. (**G**) Quantification of eosinophils in peritoneal lavage fluid of WT and *Il33*$^{-/-}$ mice treated with *N.b.* at 4 h. (n ≥ 5) Mean ± SEM, * $P < 0.05$, ** $P < 0.01$, *** $P < 0.001$, ns - not significant, Student's *t*-test.